

Gauge Symmetry and Supersymmetry Breaking From Intersecting Branes

Amit Giveon¹ and David Kutasov²

¹Racah Institute of Physics, The Hebrew University
Jerusalem 91904, Israel

²EFI and Department of Physics, University of Chicago
5640 S. Ellis Av., Chicago, IL 60637, USA

We study a system of intersecting NS and D-branes in type IIA string theory in $\mathbb{R}^{9,1}$. We show that the 3 + 1 dimensional non-supersymmetric theory at the intersection has unstable vacua which are long-lived in some regions of the parameter space of brane configurations, and disappear in others. We also comment on the relation of our construction to systems of D and \bar{D} -branes wrapped around cycles of non-compact Calabi-Yau manifolds and to other related systems.

1. Introduction

Much of the work on brane dynamics in string theory in the past decade (see *e.g.* [1,2] for reviews) focused on supersymmetric backgrounds, which are typically easier to control than generic non-supersymmetric ones. Extending the results to non-supersymmetric backgrounds is important for a number of reasons. First, they are expected to exhibit a richer set of dynamical phenomena. Second, their study might help to address the vacuum selection problem in string theory. Finally, they may be useful for constructing a model of nature below the scale of supersymmetry breaking.

In the supersymmetric case two main classes of constructions were considered in the past. One involves D-branes in the vicinity of regular or singular points on Calabi-Yau (CY) manifolds. D-branes localized near such points give rise to gauge theories some of whose properties can be analyzed using the geometric realization. One can take the CY manifold to be non-compact so that the four dimensional Newton constant vanishes, since gravity is secondary for the analysis. Of course, in order to use such constructions in realistic compactifications, they eventually have to be embedded in a compact CY.

One way to break supersymmetry in this framework is to place at a CY singularity D-branes which do not preserve any supersymmetry. Since the theory without the D-branes is supersymmetric, any instabilities associated with the lack of supersymmetry are typically relatively mild and can be resolved by rearrangement or annihilation of the branes, as is familiar from open string tachyon condensation. Recent discussions of non-supersymmetric D-brane systems on CY manifolds include [3-6].

A second class of constructions (reviewed in [1]) involves D-branes in the vicinity of Neveu-Schwarz (NS) fivebranes. These constructions are closely related to the previous ones, with the fivebranes serving as an analog of the CY geometry. When some of the directions transverse to the fivebranes are compact, the two types of constructions are related by T-duality [7-9]. Again, if one is not interested in gravitational physics, all directions transverse to the intersection of the branes can be taken to be non-compact.

In this note we will analyze some non-supersymmetric systems of intersecting D-branes and $NS5$ -branes. We will focus on systems with $3 + 1$ dimensional intersections and consider situations in which the $NS5$ -branes alone preserve some supersymmetry (as in the CY case). Adding the D-branes breaks supersymmetry and leads to potential instabilities. We would like to determine the resulting low energy dynamics as a function of the parameters of the brane configurations.

As is familiar from other brane systems, in different regions of this parameter space one can study the dynamics using different tools. In one region the correct description is in terms of a low energy gauge theory of the sort analyzed in [10].¹ In another, one can use a Dirac-Born-Infeld (DBI) action for the D-branes in the background of the fivebranes. The resulting analysis is very similar to the generalization of the Sakai-Sugimoto [16] model of dynamical chiral symmetry breaking studied in [17-19]. The main difference is that there the symmetry that is broken by the dynamics is global, while here it is a gauge symmetry. At the same time, many of the techniques that were used there can be applied here.

The plan of this paper is the following. In section 2 we introduce the brane configuration that is going to serve as our primary example and briefly discuss some of its properties. We show that already at the most elementary level of consideration, as one changes the parameters of this system, it undergoes a first order phase transition at which the nature of the vacuum changes significantly. We also discuss the gauge theory that corresponds to it at low energies.

In section 3 we study the phase structure of this system more precisely, by including the gravitational interaction between the NS and D -branes. This interaction modifies the dynamics at string tree level and can be studied by analyzing the DBI action for the D -branes in the background of the fivebranes. We find a rich structure that depends on the parameters of the brane configuration. In one region in parameter space we find a first order phase transition; in another, a second order one. We also comment on the corrections to the DBI approximation due to string (α') effects.

In section 4 we briefly describe the quantum dynamics of our brane configuration in a regime in parameter space where it is well described by a low energy gauge theory. The results of [10] imply that in this region supersymmetry, which is broken classically, is restored quantum mechanically, and the classical states discussed in section 3 are metastable. In section 5 we discuss a possible extrapolation of this picture to the regime discussed in section 3, where the gauge theory analysis is unreliable.

In section 6 we discuss our results and possible directions for further research. We also comment on the relation of our system to the brane construction relevant for the gauge theory of [10], and to the systems discussed in [5,6], which contain branes and antibranes wrapped around different cycles of CY manifolds.

¹ The brane configuration corresponding to the gauge theory of [10] was studied in [11-15]; we will comment on it below.

2. A type IIA brane configuration

2.1. Fivebranes

The starting point of our discussion is a supersymmetric configuration of $NS5$ -branes, to which we will later add D-branes that break supersymmetry. All the branes will be extended in the $\mathbb{R}^{3,1}$ labeled by (0123), the physical spacetime which will serve as the arena for the dynamics of interest. We will use two types of $NS5$ -branes, which we will refer to as NS and NS' -branes (as in [1]) and are oriented as follows:

$$\begin{aligned} NS : & \quad (012345) \\ NS' : & \quad (012389) \end{aligned} \tag{2.1}$$

It is easy to check that the branes (2.1) preserve $N = 2$ supersymmetry in 3+1 dimensions (see *e.g.* [1]). Since the directions (56) will play a special role below, we will introduce special notation for them,

$$(x^5, x^6) = (x, y) . \tag{2.2}$$

The fivebrane configuration of interest is depicted in figure 1. It includes k coincident NS -branes extended in x and localized at $y = 0$, and two NS' -branes, NS'_1 and NS'_2 , at $(x, y) = (x_1, y_1)$ and (x_2, y_2) , respectively.

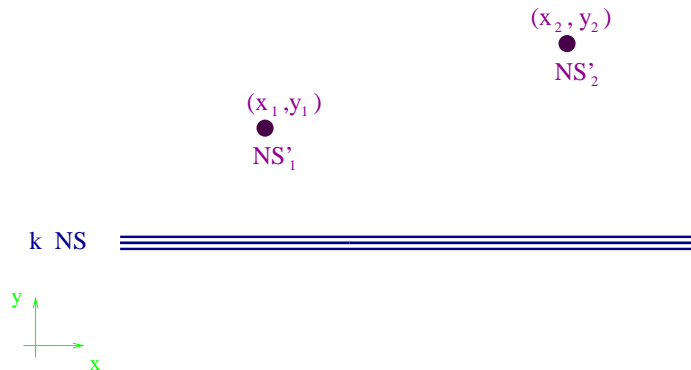


Fig. 1: The configuration of NS and NS' -branes.

For $k = 1$, each (NS, NS') intersection can be thought of as dual to a conifold singularity on a non-compact CY manifold. This description is particularly useful in the limit $y_i \ll l_s$ in which the geometry near each intersection develops a long throat. For large $\Delta x = x_2 - x_1$, the configuration of figure 1 can be thought of as describing two widely separated conifolds. As Δx decreases, the two conifolds approach each other and the geometry becomes more complicated. It can be studied using the techniques of [9].

The k coincident NS branes in figure 1 curve the geometry at the characteristic scale

$$l = \sqrt{k}l_s \tag{2.3}$$

Thus, for large k the curving of the geometry is primarily due to the NS -branes. This is one of the reasons to introduce k in the first place. We will see later that the important dynamics here is in any case due to the effect of the NS -branes so that many of the results below are valid for small k as well.

The geometry of the k NS -branes in figure 1 is given by

$$\begin{aligned} ds^2 &= dx_\mu dx^\mu + H(x^n) dx_m dx^m \\ e^{2(\Phi - \Phi_0)} &= H(x^n) \\ H_{mnp} &= -\epsilon_{mnp}^q \partial_q \Phi . \end{aligned} \tag{2.4}$$

Here $\mu = 0, 1, 2, 3, 4, 5$; $m = 6, 7, 8, 9$; H_{mnp} is the field strength of the Neveu-Schwarz B field; $g_s = \exp \Phi_0$ is the string coupling far from the fivebranes. The harmonic function H is given by

$$H(r) = 1 + \frac{kl_s^2}{r^2} = 1 + \frac{l^2}{r^2} , \tag{2.5}$$

with $r^2 = x_m x^m$. This geometry was found by C. Callan, J. Harvey and A. Strominger [20] by solving the low energy equations of motion of string theory, but these authors pointed out that due to its high degree of worldsheet supersymmetry it should not receive α' corrections. Subsequent studies in the context of Little String Theory (see *e.g.* [21,22]) have provided further support for this expectation. Thus, we will take the point of view that we can use it as long as the local string coupling is small. This is the case everywhere except in a region of (approximate) size $g_s l$ around the fivebranes.

2.2. Adding $D4$ and $\overline{D4}$ -branes

As mentioned in the introduction, a natural way to break supersymmetry is to add to the fivebrane configuration described in the previous subsection D -branes that break supersymmetry. For example, one can add N_2 $D4$ -branes stretched between the NS -branes and the NS'_2 -brane, and N_1 $\overline{D4}$ -branes stretched between the NS -branes and the NS'_1 -brane (see figure 2). We will take $N_2 \geq N_1$ below.

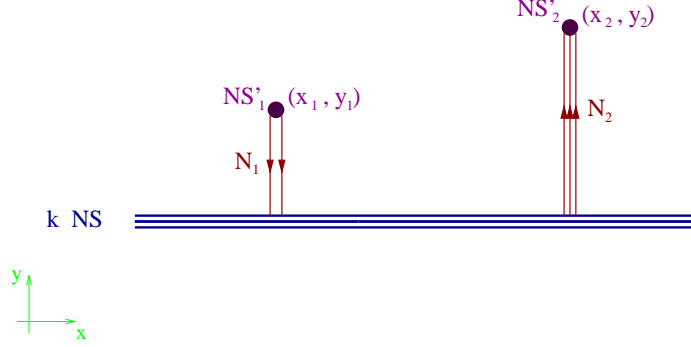


Fig. 2: The brane configuration with $D4$ and $\overline{D4}$ -branes (shown in red).

Note that the $D4$ and $\overline{D4}$ -branes in figure 2 cannot annihilate, since they carry different charges under the gauge symmetries on the two NS' -branes. This is different from systems such as that discussed in [5,6], which contains two conifold singularities some distance apart, with D -branes and \overline{D} -branes wrapping small spheres associated with the two conifolds, respectively. In that system the branes and anti-branes can annihilate after overcoming a potential barrier. We will comment on it further in section 6.

The brane configuration of figure 2 contains the free parameters (x_i, y_i) $i = 1, 2$ (which are naturally measured in units of l , (2.3)), and the string coupling g_s . In this and the next section we will study it in the (semi-) classical approximation, *i.e.* keep (x_i, y_i) fixed and send the string coupling to zero. Our purpose will be to analyze the low energy dynamics in this limit. In sections 4, 5 we will discuss g_s corrections.

The configuration of figure 2 is stable when the two NS' -branes are sufficiently far apart, but if they are close it is unstable to decay to the configuration of figure 3.

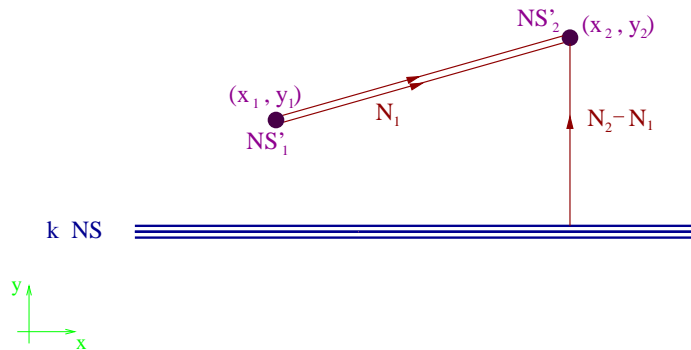


Fig. 3: A brane configuration in the same charge sector as that of figure 2.

Indeed, the difference between the energy densities of the configurations of figures 3 and 2 is (τ_4 is the tension of a $D4$ -brane)

$$V_3 - V_2 = N_1 \tau_4 \left[\sqrt{\Delta x^2 + \Delta y^2} - (y_1 + y_2) \right]. \quad (2.6)$$

This is positive for

$$\Delta x > 2\sqrt{y_1 y_2} , \tag{2.7}$$

and negative otherwise. Thus, for Δx in the range (2.7) the ground state of the system is the configuration of figure 2; otherwise it is that of figure 3. The transition between the two, at $\Delta x = 2\sqrt{y_1 y_2}$, is a first order phase transition. Indeed, as is clear from figures 2, 3, the ground state (and in particular the gauge group and massless matter content) changes abruptly across the transition.

While for $\Delta x < 2\sqrt{y_1 y_2}$ the configuration of figure 2 is not the lowest energy one, it is still locally stable. In order to make the transition to the configuration of figure 3, the ends of N_1 $D4$ and $\overline{D4}$ -branes on the NS -branes have to meet and reconnect. In the process, the energy of the D -branes increases before decreasing to that of the configuration of figure 3. Thus, in this regime the configuration of figure 2 is meta-stable (for small g_s). Naively this is true for arbitrarily small Δx (larger than the string length), but we will see later that a more careful analysis leads to different conclusions.

Similarly, for Δx in the range (2.7) the configuration of figure 3 is locally stable and is separated by a potential barrier from the actual ground state, which is the configuration in figure 2. Naively this is true for arbitrarily large Δx , but we will see later that a more careful analysis leads to different conclusions.

2.3. Gauge theory on the $D4$ -branes

In a certain region in the parameter space of the brane configuration of figure 2, the low energy dynamics is well described by the gauge theory on the $D4$ -branes. This gauge theory can be constructed as follows. Imagine starting with the configuration of figure 2 and taking the NS'_1 -brane around the NS -branes (in the x^7 direction) without varying the length of the $D4$ -branes connecting the two. At some point all the $D4$ -branes in figure 2 align, as in figure 4a, and supersymmetry is restored.

If one further takes $\Delta x = x_2 - x_1 \rightarrow 0$, one arrives at the configuration of figure 4b. For $k = 1$ this configuration corresponds to an $N = 1$ supersymmetric gauge theory with gauge group

$$U(N_1) \times U(N_2) , \tag{2.8}$$

and bifundamental chiral superfields Q, \tilde{Q} . For $k > 1$ there is also an adjoint of the gauge group (2.8), Φ , with a polynomial superpotential [1].

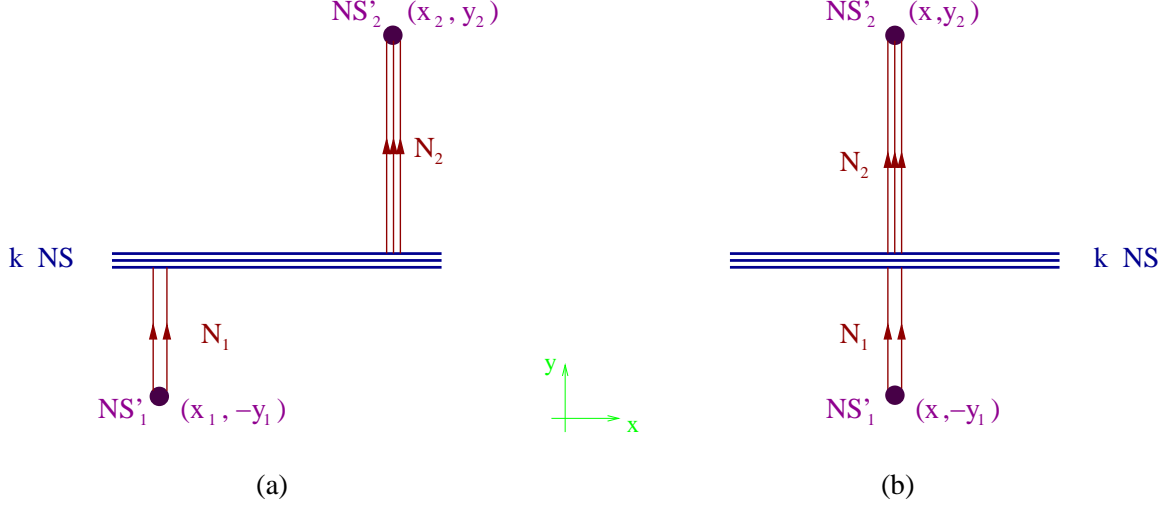


Fig. 4: The brane configuration corresponding to the electric gauge theory, with non-vanishing (a), and vanishing (b) mass for the bifundamentals.

The gauge couplings of $U(N_1)$ and $U(N_2)$, g_1 and g_2 , are given as usual by

$$g_i^2 = \frac{g_s l_s}{y_i} . \quad (2.9)$$

In particular, by varying the distances y_i one can change the relative strength of the two couplings. E.g. in the limit $y_2 \rightarrow \infty$, $U(N_2)$ becomes a global symmetry and the theory becomes SQCD with gauge group $U(N_1)$ and N_2 flavors in the fundamental representation.

As is standard in constructions of this sort [1], deformations of the brane configuration of figure 4b correspond to parameters in the gauge theory (2.8). For example, displacing the two NS' -branes relative to each other in the x direction by an amount Δx , as in figure 4a, corresponds to turning on a quadratic superpotential for the bifundamentals,

$$W = m\tilde{Q}Q \equiv mM , \quad (2.10)$$

where M is the meson field, and the mass m is given by

$$m = \frac{\Delta x}{2\pi\alpha'} . \quad (2.11)$$

Relative displacements between the NS' -branes and the NS -brane in x^7 correspond to Fayet-Iliopoulos D-terms in the $U(1)$ factors of the gauge group (2.8). Reconnecting some of the $D4$ -branes in figure 4b such that they stretch between the two NS' -branes and moving them off in the (89) directions corresponds to giving an expectation value to the meson field M along one of its flat directions.

From the point of view of the brane configuration of figure 4, configurations in which the two NS' -branes are on the same side of the NS -brane, as in figures 2, 3, are obtained [23,24] by applying Seiberg duality to the $U(N_1)$ factor in (2.8). Indeed, starting with figure 4b and performing the opposite move to the one that led us to it, namely taking the NS'_1 -brane around the NS -brane in x^7 until it hits the $D4$ -branes stretched between the NS and NS'_2 -branes, leads² to the configuration of figure 5.

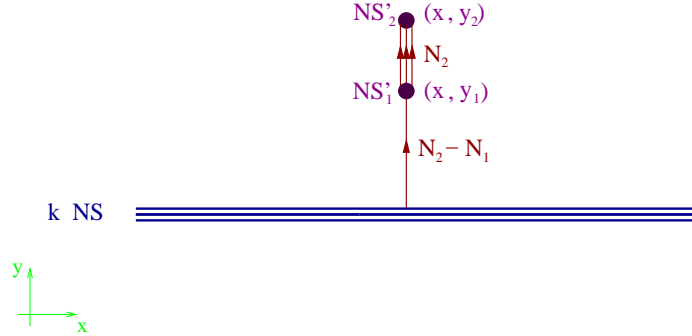


Fig. 5: The brane configuration corresponding to the magnetic gauge theory.

The corresponding gauge theory has gauge group

$$U(N_2 - N_1) \times U(N_2) , \quad (2.12)$$

bifundamental “quarks” q, \tilde{q} , and an adjoint of $U(N_2)$, M (related to the electric mesons (2.10)), coupled to the quarks via a cubic superpotential

$$W_{\text{mag}} = \frac{1}{\Lambda} M \tilde{q} q , \quad (2.13)$$

where Λ is an energy scale. This is precisely the matter content and interactions of the Seiberg dual [25] of (2.8). Configurations such as those of figures 2,3 are obtained by turning on the superpotential (2.10), which in the magnetic language corresponds to adding a term linear in M to the superpotential (2.13),

$$W_{\text{mag}} = \frac{1}{\Lambda} M \tilde{q} q + m M . \quad (2.14)$$

One can of course go directly from the brane configuration of figure 2 to that of figure 5 without passing through the “electric” configurations of figure 4. Indeed, taking the

² After the annihilation of N_1 branes and antibranes by open string tachyon condensation.

separation Δx (or equivalently, (2.11), the parameter m in (2.14)) in figure 2 to zero leads precisely to figure 5.

Conversely, one can think of the brane configurations of figures 2, 3 as particular states in the magnetic gauge theory with gauge group (2.12) and superpotential (2.14). Of course, the gauge theory description is only valid at low energies. This means that the mass parameter m and thus the separation of NS' -branes Δx (2.11) must be sufficiently small for this description to be valid. If m is too large, the relevant description is not the gauge theory one, but rather that of the UV completion of the theory via brane dynamics in string theory.

We will return to the gauge theory described above in section 4. We will see that it is closely related to the theory studied in [10], and in particular has meta-stable supersymmetry breaking vacua. Our main motivation is to understand how the analysis of [10] ties in with the behavior of the brane system under consideration in other regimes in parameter space, where one needs to use other techniques for studying it.

3. DBI analysis

In section 2 we discussed the brane configurations of figures 2 – 5 in the classical, flat space limit, in which the fivebranes are treated as hypersurfaces on which D-branes can end. For a more accurate description one needs to take into account certain classical and quantum (g_s) corrections. In this section we will discuss the former; the latter will be discussed later in the paper.

3.1. General analysis

The main source of classical corrections is the gravitational potential created by the k NS -branes (2.4), (2.5), and its effects on the $D4$ -branes. One reason for including it in the analysis has to do with the transition between the configurations of figures 2 and 3 which, as discussed in section 2, occurs as we vary the parameters of the brane configuration. This transition takes place near the NS -branes where the geometry (2.4) is nontrivial. Another reason is that while the discussion of section 2.2 might be expected to be reliable for large separations of the branes³, the fivebrane geometry gives large corrections when the parameters y_i in figures 2, 3 are comparable to l (2.3).

³ Although we will see that even in that regime the fivebrane geometry gives rise to important new qualitative effects.

We will describe the D-branes by a DBI action in the NS -brane background (2.4). This description is reliable for large k but some aspects of it are valid for all k . We will comment on this issue later in the section.

The straight brane configuration of figure 2 is a solution of the DBI equations of motion for all values of l . In the configuration of figure 3, the geometry (2.4) gives rise to an attractive force that pulls the N_1 $D4$ -branes stretched between the NS' -branes towards the NS -branes. To calculate their shape one needs to analyze the DBI action for $D4$ -branes in the geometry (2.4) (see [26] for a related discussion).

We are looking for a solution in which the $D4$ -branes are described by a smooth curve $y = y(x)$ connecting the points (x_1, y_1) and (x_2, y_2) . Its shape is obtained by extremizing the DBI action

$$\mathcal{S}_4 = -N_1 \tau_4 \int dx \frac{1}{\sqrt{H(y)}} \sqrt{1 + H(y)(\partial_x y)^2} = -N_1 \tau_4 \int dx \sqrt{\frac{1}{H(y)} + (\partial_x y)^2}, \quad (3.1)$$

where $H(y)$ is given by (2.5). The equations of motion of this action have a first integral

$$H(y) \sqrt{\frac{1}{H(y)} + (\partial_x y)^2} = C. \quad (3.2)$$

To solve (3.2) it is useful to think about the qualitative form of the solution as a function of

$$\Delta x = x_2 - x_1. \quad (3.3)$$

For $\Delta x = 0$, figure 3 reduces to figure 5 and the N_1 $D4$ -branes connecting the NS' -branes stretch vertically, along the y direction. For non-zero Δx , the solution is a deformation of the N_1 straight branes in figure 3. If Δx is small enough, y is a monotonic function of x everywhere. This regime can be studied using the methods below, but we will not describe it in detail here.

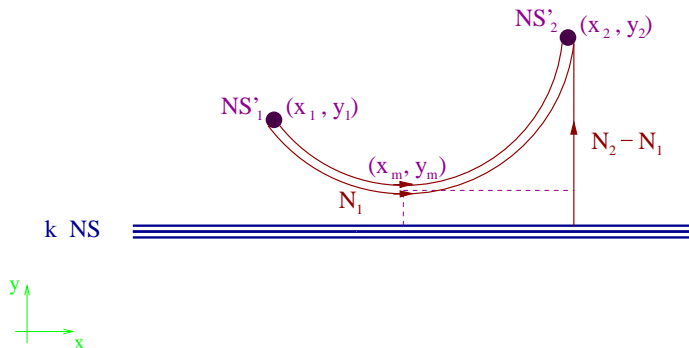


Fig. 6: The effect of the gravitational attraction to the NS -branes on the $D4$ -branes in figure 3.

When Δx exceeds a certain critical value (which can be extracted from the formulae below) the branes take the qualitative form in figure 6. In particular, the minimal value of y , y_m , is attained at a point x_m along the curve, $x_1 < x_m < x_2$. In this regime, which we will focus on here, the constant C in (3.2) is given by the value of the harmonic function (2.5) at y_m ,

$$C^2 = H(y_m) . \quad (3.4)$$

Applying the first order differential equation (3.2) to the two intervals $x_1 \leq x \leq x_m$ and $x_m \leq x \leq x_2$ leads to the following two relations between the parameters in figure 6:

$$\begin{aligned} \int_{y_m}^{y_1} \frac{dy H(y)}{\sqrt{H(y_m) - H(y)}} &= x_m - x_1 , \\ \int_{y_m}^{y_2} \frac{dy H(y)}{\sqrt{H(y_m) - H(y)}} &= x_2 - x_m . \end{aligned} \quad (3.5)$$

The integrals in (3.5) can be performed exactly. One finds

$$\begin{aligned} \frac{y_m}{l} \sqrt{y_1^2 - y_m^2} + l\theta_1 &= x_m - x_1 , \\ \frac{y_m}{l} \sqrt{y_2^2 - y_m^2} + l\theta_2 &= x_2 - x_m , \end{aligned} \quad (3.6)$$

where $\theta_i \in [0, \frac{\pi}{2}]$, and

$$\cos \theta_i = \frac{y_m}{y_i} . \quad (3.7)$$

Adding the two equations (3.6) and using (3.7) gives the following relation between Δx and y_m :

$$\Delta x = x_2 - x_1 = \frac{1}{2l} (y_1^2 \sin 2\theta_1 + y_2^2 \sin 2\theta_2) + l(\theta_1 + \theta_2) . \quad (3.8)$$

The energy of the configuration of figure 6 is given by (minus) the action (3.1),

$$E_{\text{curved}} = N_1 \tau_4 \int dx \sqrt{\frac{1}{H(y)} + (\partial_x y)^2} . \quad (3.9)$$

Performing the integral in (3.9), using (3.2), (3.4), one finds

$$E_{\text{curved}} = N_1 \tau_4 \frac{\sqrt{H(y_m)}}{2l} (y_1^2 \sin 2\theta_1 + y_2^2 \sin 2\theta_2) . \quad (3.10)$$

To get a sense of the behavior described by equations (3.8), (3.10) we will next discuss in some detail the special case $y_1 = y_2 = y$, and comment on the generalization to arbitrary $y_2 \geq y_1$.

3.2. $y_1 = y_2 = y$

In this case the two NS' -branes in figures 2, 6 are at the same distance from the NS -branes. Equation (3.8) simplifies to

$$\Delta x = \frac{y^2}{l} \sin 2\theta + 2l\theta , \quad (3.11)$$

with (3.7)

$$\cos \theta = \frac{y_m}{y} . \quad (3.12)$$

The angle θ provides a parametrization of y_m in figure 6. As it increases from 0 to $\pi/2$, y_m decreases from y to 0. Thus, the relation (3.11) can be viewed as determining y_m in terms of Δx . It turns out to be useful to discuss the form of the solution separately for $y < l$ and $y > l$.

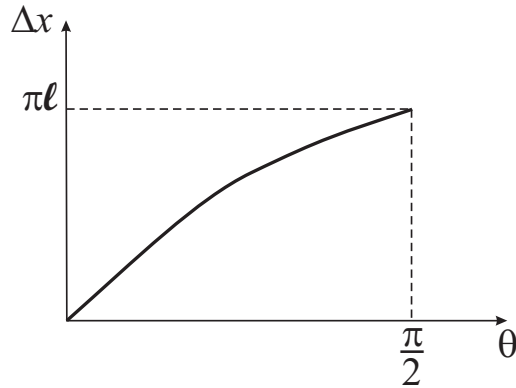


Fig. 7: A plot of the function (3.11) for $l = \sqrt{2}y$.

3.2.1. $y < l$:

In this case the function (3.11), which is plotted in figure 7 for the special case $l = \sqrt{2}y$, is monotonically increasing. For $\theta \rightarrow 0$ (*i.e.* $y_m \rightarrow y$) it approaches $\Delta x = 0$, while for $\theta \rightarrow \pi/2$ ($y_m \rightarrow 0$) it approaches $\Delta x = \pi l$. In particular, in this case there are two distinct regimes:

- (1) $0 < \Delta x < \pi l$, where there are two solutions of the equations of motion for the $D4$ -branes: the straight brane solution of figure 2 and the curved brane one of figure 6.
- (2) $\Delta x \geq \pi l$, where the curved brane solution of figure 6 does not exist, and the only allowed configuration is that of figure 2.

In regime (1) one needs to determine the true ground state, *i.e.* to find which of the two allowed configurations has lower energy. The energy of the $D4$ -branes in figure 2 is given by the flat space result

$$E_{\text{straight}} = N_1 \tau_4 2y . \quad (3.13)$$

For the configuration of figure 6 we have

$$E_{\text{curved}} = \frac{N_1 \tau_4}{l} \sqrt{H(y_m)} y^2 \sin 2\theta = N_1 \tau_4 2y \sqrt{H(y_m)} \frac{y_m}{l} \sin \theta . \quad (3.14)$$

Dividing the two we find

$$\left(\frac{E_{\text{curved}}}{E_{\text{straight}}} \right)^2 = \left[1 + \left(\frac{y_m}{l} \right)^2 \right] \left[1 - \left(\frac{y_m}{y} \right)^2 \right] < 1 . \quad (3.15)$$

Thus, we see that for $y < l$, the configuration of figure 6 has lower energy than the straight brane of figure 2, whenever it exists, *i.e.* for all $\Delta x < \pi l$. This means that if we start with the configuration of figure 2 with $\Delta x < \pi l$, and continuously deform it⁴ in the direction of figure 6, the energy decreases, until it reaches that of figure 6. If we continue to deform it further, the energy increases again.

One can describe the situation qualitatively by the potential in figure 8. The horizontal axis in that figure corresponds to one of the many possible deformations of the shape of the $D4$ -brane. For example, one can think of it as labeling the smallest value of y reached by the $D4$ -branes. The configuration of figure 2 corresponds to the local maximum at the extreme left of figure 8, while that of figure 6 corresponds to the global minimum of the plot. As Δx increases, this minimum moves to the left until, at $\Delta x = \pi l$ it coincides with the local maximum at the extreme left. Conversely, as Δx decreases, the minimum moves to the right, and as $\Delta x \rightarrow 0$ it approaches the boundary at the extreme right of the plot, which corresponds to $\theta = 0$ in (3.11) or equivalently to $y_m = y$.

⁴ In doing this, it is useful to think of N_1 of the $D4$ -branes in figure 2 as starting at the NS'_1 -brane, going down to the NS -branes, proceeding along the NS -branes and then back up to the NS'_2 -brane. The segment that runs along the NS -branes is massless to leading order in g_s .

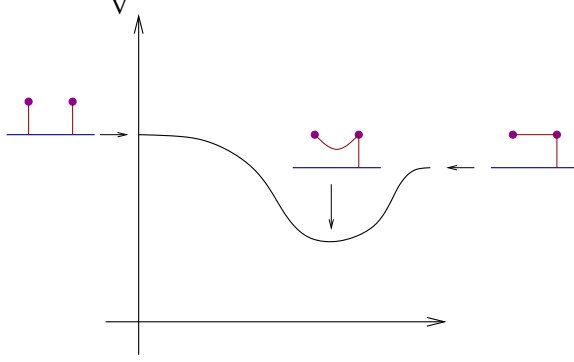


Fig. 8: The qualitative behavior of the potential for the $D4$ -branes for $\Delta x < \pi l$.

We see that for $\Delta x < \pi l$ the configuration of figure 2 is an unstable equilibrium, *i.e.* it contains a tachyonic mode. Above we presented this mode as a geometric instability of the brane configuration of figure 2 to deformations that take it towards that of figure 6. One might feel uncomfortable with that presentation since it involves the behavior of $D4$ -branes arbitrarily close to the NS -branes, deep in the strong coupling region near the fivebranes.

There is another, related, way of thinking about this instability, which avoids this difficulty. It involves the dynamics of a fundamental string stretched between the $D4$ and $\overline{D4}$ -branes in figure 2. Since this string is stretched between a brane and an anti-brane, it satisfies the opposite GSO projection from strings both of whose ends lie on D -branes with the same charge. In particular, its lowest lying excitation is the open string tachyon.

The mass squared of this tachyon receives a negative contribution from the zero point energy of the string and a positive one from the stretching of the string over a distance Δx . In the flat space approximation of figure 2, if $\Delta x > \sqrt{2}\pi l_s$ the tachyon is massive. We assumed above that $\Delta x < \pi l$, but since l (2.3) can in general be much larger than l_s , it appears that there should be no instability associated with this tachyon, at least for $\pi l > \Delta x > \sqrt{2}\pi l_s$.

In fact, the situation is more interesting. The $D4$ and $\overline{D4}$ -branes in figure 2 are stretched vertically from $y = y_1 = y_2$ all the way down to $y = 0$. The effective mass of the open string tachyon T , m_T , depends on position along the branes. Deep inside the fivebrane throat, *i.e.* for $y \ll l$, it can be computed by using the near-horizon geometry of the fivebranes, which is a linear dilaton space. The result is

$$(2\alpha' m_T)^2 = \left(\frac{\Delta x}{\pi}\right)^2 - l^2 . \quad (3.16)$$

The first term on the r.h.s. is due to stretching of the string in the x direction. The second provides a constant shift proportional to k . The derivation of equation (3.16) is very similar to that of equation (5.2) in [27].

For comparison,⁵ the mass of the open string tachyon in flat spacetime with constant dilaton is

$$(2\alpha' m_T)^2 = \left(\frac{\Delta x}{\pi} \right)^2 - 2l_s^2. \quad (3.17)$$

Equation (3.16) implies that for $\Delta x < \pi l$, the open string tachyon stretched between the branes and anti-branes in figure 2 gives rise to a localized instability of the brane configuration of figure 2. Its condensation leads to the configuration of figure 6.

For $\Delta x > \pi l$ the open string tachyon is massive everywhere, and the configuration of figure 2 is locally stable. In fact, as we have seen, it is the global ground state of the system in this regime (at least classically).

Some comments are in order at this point:

- (1) When the asymptotic string coupling is very small, there is a wide range of distances in which the geometry (2.4) reduces to a linear dilaton one, and the local string coupling is still small. Thus, the instability of the configuration of figure 2 for $\Delta x < \pi l$ can be seen at open string tree level.
- (2) We have given above two descriptions of the instability of the configuration of figure 2 to decay to that of figure 6. One is purely geometric, associated with the discussion of figure 8. The other involves the condensation of the tachyon stretched between branes and anti-branes. In fact the two descriptions are known to be related. In the near-horizon geometry of the fivebranes this is the duality between the hairpin brane of [30] and the boundary $N = 2$ Liouville model (or boundary Sine-Liouville in the bosonic case), which was discussed in the bosonic case in [30,31] and in the fermionic case relevant for our analysis in [32]. Our results suggest that this duality can be extended to the full fivebrane geometry (2.4).
- (3) The discussion of the open string tachyon above is very reminiscent of the study of non-supersymmetric deformations of the CHS geometry in [27]. In fact, in the throat of the fivebranes it is a direct open string analog of that system. As usual, in going from closed to open strings the instability becomes easier to analyze and the endpoint of tachyon condensation easier to identify.

⁵ The fact that the two masses coincide for $k = 2$ NS -branes seems to be related to observations in [28,29].

To summarize, for $y < l$, as we vary Δx the system undergoes a phase transition. For $\Delta x < \pi l$, the configuration of figure 2 (which corresponds to the unbroken phase) is unstable, and the stable one is that of figure 6. The order parameter can be taken to be the expectation value of the tachyon T stretched between the branes and the anti-branes. It transforms in the bifundamental representation of the gauge group on the branes (2.8), and is non-zero in this regime. The gauge symmetry is broken,

$$U(N_1) \times U(N_2) \rightarrow U(N_1)_{\text{diag}} \times U(N_2 - N_1) . \quad (3.18)$$

As Δx increases, the order parameter $\langle T \rangle$ decreases; it goes to zero as $\Delta x \rightarrow \pi l$. For $\Delta x > \pi l$ the order parameter vanishes and the theory is in the unbroken phase, with the full gauge symmetry (2.8) realized. Thus, the system exhibits a second order phase transition at $\Delta x = \pi l$. The behavior of the order parameter is schematically depicted in figure 9.

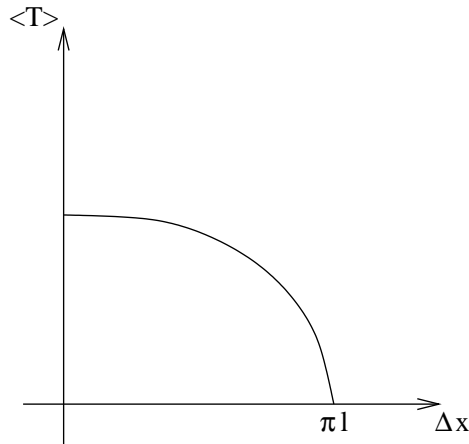


Fig. 9: The qualitative behavior of the order parameter for $y < l$.

Geometrically, for small Δx the ground state is the configuration of figure 6 with y_m slightly below y . As Δx increases, the curved $D4$ -brane dips further and further towards the fivebranes, and as $\Delta x \rightarrow \pi l$ it continuously approaches the straight brane configuration of figure 2. For larger Δx the configuration of figure 2 is the only possible one and is thus the ground state of the system.

We stress again that the discussion above is classical. We will see later that g_s corrections may lead to additional vacua with unbroken supersymmetry, to which all the states described here can decay. Nevertheless, for small g_s the picture we arrived at provides a very good approximation to the physics of these states for a very long period of time.

3.2.2. $y > l$:

Looking back at equation (3.11), it is easy to see that in this case Δx is not a monotonic function of θ (see figure 10). It has a maximum at $\theta = \theta_0$, with

$$\cos 2\theta_0 = -\frac{l^2}{y^2} . \quad (3.19)$$

Note that $\frac{\pi}{4} < \theta_0 < \frac{\pi}{2}$. The value of y_m (3.12) corresponding to (3.19) is

$$2y_m^2 = y^2 - l^2 . \quad (3.20)$$

Plugging this into (3.11), (3.12) one can calculate the largest Δx , Δx_m , for which a smooth solution exists. For $y \gg l$ it is given by

$$\Delta x_m \approx \frac{y^2}{l} . \quad (3.21)$$

This should be compared to the case $y < l$, where we found that $\Delta x_m = \pi l$. Like there, for $\Delta x > \Delta x_m$ there is a unique solution to the DBI equations of motion – the configuration of figure 2. For $\Delta x < \Delta x_m$ the structure is more intricate than before, and our next goal is to elucidate it.

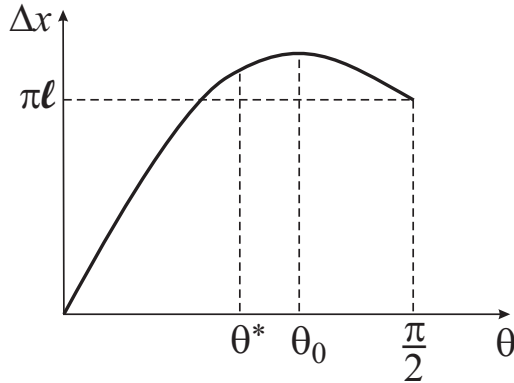


Fig. 10: A plot of the function (3.11) for $y = \sqrt{2}l$.

We start with the region $0 < \Delta x < \pi l$. From figure 10 we see that the DBI equations of motion have in this case a unique smooth solution, and we expect its energy to be lower than that of the straight brane solution of figure 2. The reason for that was explained in subsection 3.2.1, where we pointed out that the open string tachyon gives rise in this regime to an instability of the configuration of figure 2, which is localized in the near-horizon region

of the fivebranes. Condensation of this tachyon should lead to the configuration of figure 6, which therefore should have lower energy.

To check this, we need to show that the ratio of energies in equation (3.15) is smaller than one. One can rewrite this ratio as

$$\left(\frac{E_{\text{curved}}}{E_{\text{straight}}}\right)^2 = \left[1 + \left(\frac{y}{l}\right)^2 \cos^2 \theta\right] \sin^2 \theta, \quad (3.22)$$

and note that it has the following properties:

- (1) It grows with θ in the range $0 < \theta < \theta_0$, where θ_0 (3.19) is the value corresponding to Δx_m (3.21). For $\theta > \theta_0$ the ratio (3.22) starts decreasing.
- (2) It is equal to one for $\theta = \theta^*$, with

$$\sin \theta^* = \frac{l}{y}. \quad (3.23)$$

By comparing (3.23) to (3.19) one finds that $\theta^* < \theta_0$.

- (3) At $\theta = \theta^*$, $\Delta x > \pi l$. Indeed, plugging (3.23) into (3.11) we find that for $\theta = \theta^*$

$$\frac{\Delta x}{l} = 2(\cot \theta^* + \theta^*). \quad (3.24)$$

The r.h.s. of (3.24) is a monotonically decreasing function of θ^* . It is equal to π for $\theta^* = \pi/2$, and for all other $\theta^* \in (0, \frac{\pi}{2})$ it is larger. This establishes that for $\Delta x < \pi l$ the smooth curved solution of the DBI equations of motion has lower energy than the straight brane configuration of figure 2, as expected.

Having understood the region $\Delta x < \pi l$ we move on to $\Delta x > \pi l$. According to figure 10, in this regime a second smooth solution to the DBI equations of motion appears, at a larger value of θ , *i.e.* a smaller value of y_m (see (3.12)). We will denote the values of θ (3.12) that correspond to the two solutions of (3.11) by θ_S and θ_L , respectively, where by definition

$$\theta_S \leq \theta_L, \quad (3.25)$$

i.e. θ_S is the smaller of the two.

The fact that there are two solutions in this regime is simple to understand from the preceding discussion. For $\Delta x > \pi l$, the open string tachyon stretched between the $D4$ and $\overline{D4}$ -branes in figure 2 is massive (see (3.16)). Thus, this brane configuration is locally stable. However, if Δx is only slightly larger than πl it is not globally stable since, as we have seen by analyzing the ratio (3.22), the energy density of the configuration of figure 6

is smaller than that of figure 2 for all $\theta < \theta^*$ (3.23), which includes a finite range of Δx 's larger than πl .

Therefore, if we start with the configuration of figure 2 and deform it towards that of figure 6, we expect the energy to increase, reach a maximum and then decrease to that of the global minimum, the stable configuration of figure 6. The maximum of the energy between the two minima corresponds to the second solution seen in figure 10. We can describe the energetics by the qualitative plot in figure 11.

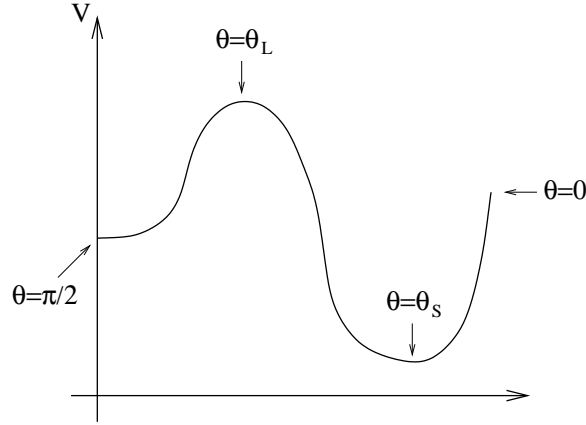


Fig. 11: The qualitative behavior of the potential for the $D4$ -branes for $\Delta x > \pi l$, $\theta_S < \theta^*$.

As is clear from this figure, the energy of the solution with $\theta = \theta_L$ must be larger than that of the straight brane configuration of figure 2 and than that of the solution with $\theta = \theta_S$. Both of these expectations can be verified using the formulae above.

The fact that the energy of the configuration with $\theta = \theta_L$ is larger than that of the one of figure 2 follows from our discussion of the ratio (3.22) above. We mentioned that this ratio increases for $0 < \theta < \theta_0$ and decreases for $\theta_0 < \theta < \pi/2$. Since $\theta_L > \theta_0$, the value of the ratio (3.22) at $\theta = \theta_L$ is larger than at $\theta = \pi/2$. The latter is equal to one (essentially by definition); therefore, the former is larger than one.

To prove that the energy for θ_L is larger than that for θ_S one can proceed as follows. From (3.22) we see that we need to prove the inequality

$$\sin^2 \theta_S + \left(\frac{y}{2l}\right)^2 \sin^2 2\theta_S \leq \sin^2 \theta_L + \left(\frac{y}{2l}\right)^2 \sin^2 2\theta_L . \quad (3.26)$$

This is equivalent to

$$\cos 2\theta_S + \left(\frac{y}{2l}\right)^2 \cos 4\theta_S \geq \cos 2\theta_L + \left(\frac{y}{2l}\right)^2 \cos 4\theta_L . \quad (3.27)$$

Rearranging this inequality and using a trigonometric identity for the difference of cosines gives

$$\sin(\theta_S + \theta_L) \sin(\theta_L - \theta_S) \geq - \left(\frac{y}{2l} \right)^2 \sin[2(\theta_S + \theta_L)] \sin[2(\theta_L - \theta_S)] . \quad (3.28)$$

Using the doubling formula for sine and the fact that $\theta_S + \theta_L$ is between 0 and π so $\sin(\theta_L \pm \theta_S)$ is positive, gives

$$1 \geq - \left(\frac{y}{l} \right)^2 \cos(\theta_S + \theta_L) \cos(\theta_L - \theta_S) . \quad (3.29)$$

We also need to use the fact that θ_S and θ_L correspond to the same Δx (3.11). This means that

$$\left(\frac{y}{l} \right)^2 \cos(\theta_S + \theta_L) \frac{\sin(\theta_L - \theta_S)}{\theta_L - \theta_S} = -1 . \quad (3.30)$$

Plugging this in (3.29) we conclude that we need to prove that

$$(\theta_L - \theta_S) \cot(\theta_L - \theta_S) \leq 1 . \quad (3.31)$$

Equivalently, we need to show that

$$f(\theta) = \tan \theta - \theta \quad (3.32)$$

is positive for $\theta = \theta_L - \theta_S \in (0, \frac{\pi}{2})$. This is indeed the case, since f vanishes at $\theta = 0$ and its derivative is positive for all $\frac{\pi}{2} > \theta > 0$.

The above checks substantiate the picture suggested by figure 11 for $\Delta x > \pi l$ but sufficiently small such that $\theta_S < \theta^*$ (3.23). As we increase Δx beyond that point, we get to a regime where, as we have seen, the energy of the straight brane configuration of figure 2 is lower than that of the smooth curved solution to the DBI equations of motion. In this regime, the potential has the qualitative structure depicted in figure 12.

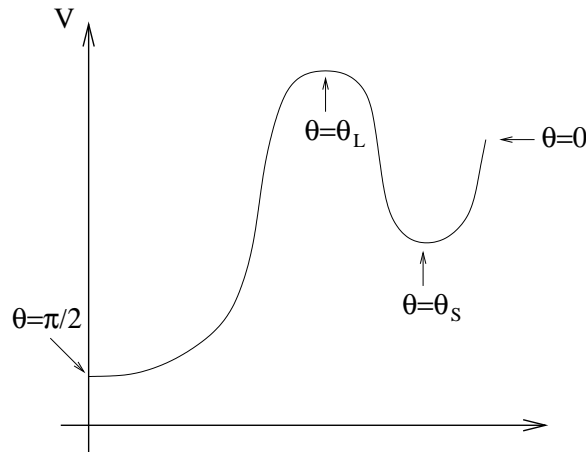


Fig. 12: The qualitative behavior of the potential for the $D4$ -branes for $\Delta x > \pi l$, $\theta_0 > \theta_S > \theta^*$.

Thus, for $\theta_S < \theta^*$ (or small Δx) the classical ground state of the system corresponds to a brane configuration of the type of figure 6. The gauge symmetry is broken as in (3.18), and the corresponding order parameter, the expectation value of the bifundamental tachyon, is non-zero. On the other hand, for $\theta_S > \theta^*$ (sufficiently large Δx), the ground state is the configuration of figure 2, the order parameter vanishes, and the gauge symmetry is unbroken.

The transition between the two regimes at $\theta = \theta^*$ is a first order phase transition. The order parameter jumps discontinuously from a non-zero value to zero as we pass that point (see figure 13).

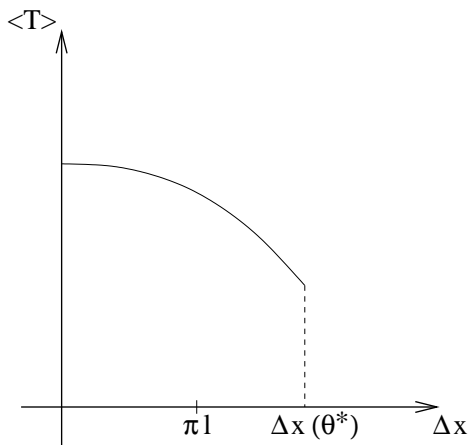


Fig. 13: The qualitative behavior of the order parameter for $y > l$.

For $\theta_0 > \theta_S > \theta^*$, the broken vacuum remains a local minimum of the potential and is a meta-stable state at weak string coupling. As we increase θ_S (or Δx), the local minimum at θ_S and local maximum at θ_L approach each other, and the meta-stable state with broken symmetry becomes less stable. Eventually, at a value of Δx corresponding to $\theta_S = \theta_L = \theta_0$, the meta-stable minimum and local maximum meet and for larger values of Δx the equations of motion no longer have a smooth curved solution of the kind drawn in figure 6.

It is instructive to compare the preceding discussion to the one of section 2.2, where we effectively took $l \rightarrow 0$. There, we found a transition at (2.7) $\Delta x = 2y$. Here, the transition was found to occur at $\theta = \theta^*$ (3.23). To compare to section 2 we need to take $y \gg l$, and plugging this into (3.23), (3.11) we find the same answer as there. An important qualitative difference with respect to the analysis of section 2 is that there the broken vacuum of figure 3 appeared to be a meta-stable state for arbitrarily large Δx . The

more accurate analysis of this section revealed that this is true for $\Delta x < y^2/l$ (3.21), but beyond that point the meta-stable broken vacuum state ceases to exist. This is consistent with the discussion of section 2, since the upper bound (3.21) goes to infinity as $l \rightarrow 0$.

3.3. General y_1, y_2

In this subsection we comment on the generalization of the results of the previous subsection to arbitrary $y_1 \leq y_2$, for which the relation between Δx and y_m in figure 6 is given by eq. (3.8). In subsection 3.2 we found it convenient to parametrize y_m via the angle θ (3.12). The natural analog of θ in the general case is θ_1 in (3.7). As this angle varies between 0 and $\pi/2$, y_m varies between y_1 and 0, respectively. The latter case corresponds to the geometry of figure 2. The angle θ_2 , which appears in equation (3.8), can be expressed in terms of θ_1 using (3.7) as

$$\cos \theta_2 = \frac{y_1}{y_2} \cos \theta_1 . \quad (3.33)$$

The resulting function $\Delta x(\theta_1)$ (3.8) is a natural generalization of (3.11) to arbitrary $y_1 \leq y_2$. Its values at the boundaries $\theta_1 = 0, \pi/2$ are the following. For $\theta_1 = \theta_2 = \pi/2$, one finds $\Delta x = \pi l$ (this is the configuration of figure 2, which of course exists for all Δx , but is only obtained as a limit of a smooth solution to the DBI equations of motion as $\Delta x \rightarrow \pi l$). The value of Δx for $\theta_1 = 0$, which corresponds to $y_m = y_1$, depends on y_2 , and grows linearly with y_2 for large values of the latter. Large y_2 and small Δx is an example of a regime (mentioned in section 3.1) in which $y(x)$ is monotonic. We will not study this regime here.

As in subsection 3.2, it is interesting to determine whether the function $\Delta x(\theta_1)$ is monotonic in its regime of validity. A short calculation shows that it is monotonically increasing for

$$y_1 y_2 < l^2 . \quad (3.34)$$

For $y_1 y_2 > l^2$ it has a maximum at

$$\cos(\theta_1 + \theta_2) = -\frac{l^2}{y_1 y_2} . \quad (3.35)$$

These results generalize those found in the previous subsection for the case $y_1 = y_2 = y$. In particular, (3.35) is the analog of (3.19) for general y_1, y_2 .

As before, it is useful to discuss separately the regime (3.34) and its complement. Much of the analysis is similar to that of subsection 3.2, so we will be brief.

3.3.1. $y_1 y_2 < l^2$

For $\Delta x > \pi l$ there is again a unique solution to the equations of motion, corresponding to the straight branes of figure 2. For $\Delta x < \pi l$ there are two solutions, those of figures 2 and 6, and we need to compare their energies. For reasons that were explained in the previous subsection, we expect the smooth, curved solution of figure 6 to be the true classical ground state in this case. To show this, we must prove that (see (3.10))

$$\frac{1}{2l} \sqrt{H(y_m)} (y_1^2 \sin 2\theta_1 + y_2^2 \sin 2\theta_2) < y_1 + y_2 . \quad (3.36)$$

Using (3.7), this can be rewritten as

$$F(y_m) < y_1 + y_2 , \quad (3.37)$$

where

$$F(y_m) = \sqrt{1 + \frac{y_m^2}{l^2}} \left(\sqrt{y_1^2 - y_m^2} + \sqrt{y_2^2 - y_m^2} \right) . \quad (3.38)$$

To see that the inequality (3.37) is indeed correct, one notes that it becomes an equality for $y_m = 0$ (by construction), and for any larger y_m the function (3.38) is smaller since the derivative $\frac{dF}{dy_m}$ is negative. Thus, we conclude that, as expected, for $\Delta x < \pi l$ the configuration of figure 2 is unstable to the condensation of the tachyon discussed in the previous subsection, whose mass is given by (3.16), and the stable configuration is that of figure 6.

As $\Delta x \rightarrow \pi l$, the configuration of figure 6 approaches that of figure 2, and for larger Δx there is a unique vacuum. The system undergoes a second order phase transition at $\Delta x = \pi l$, as in figure 9.

3.3.2. $y_1 y_2 > l^2$

We expect a similar picture to that of subsection 3.2. For $\Delta x < \pi l$ there should be a unique smooth curved solution to the DBI equations of motion. For Δx slightly above πl a second solution with $y_m \ll y_1, y_2$ should appear. This solution should be a local maximum of the energy, separating the global minimum of figure 6 from the local one (figure 2).

The appearance of a solution with small y_m can be verified directly as follows. Equation (3.7) implies that

$$\theta_i = \frac{\pi}{2} - \frac{y_m}{y_i} + O(y_m^2) . \quad (3.39)$$

Plugging this into (3.8) one finds

$$\Delta x = \pi l + y_m \left(\frac{y_1}{l} + \frac{y_2}{l} - \frac{l}{y_1} - \frac{l}{y_2} \right) + O(y_m^2). \quad (3.40)$$

The expression in brackets in (3.40) is positive for $y_1 y_2 > l^2$, so when Δx is slightly larger than πl , the solution for y_m is small, as expected. In order to show that this solution is a local maximum of the energy, one has to check that the function $F(y_m)$ (3.38) satisfies $F(y_m) > y_1 + y_2$. It is easy to check that this is indeed the case to leading order in y_m .

The general picture in this case is expected to be very similar to that of subsection 3.2.2. For Δx slightly above πl , the straight brane configuration of figure 2 is a local minimum of the energy, while the true ground state is a curved configuration as in figure 6. As Δx increases, the relative energies of the two minima change, until when the inequality (3.37) becomes an equality, they flip and the straight brane configuration becomes the ground state. The configuration of figure 6 remains a local minimum until a much larger value of Δx , above which it ceases to exist. We will leave a more detailed investigation to future work.

3.4. Finite k corrections

The analysis of this section so far involved two types of approximations. First, we used the supergravity result for the fivebrane geometry, (2.4). In principle there can be perturbative and non-perturbative α' corrections to the background. Second, we used the DBI approximation to describe the D-branes, and again in general one expects corrections to this description. For large k , both of these approximations are justified, but one can ask what happens for finite k . In this subsection we briefly comment on this issue.

Some features of our description are known not to receive α' corrections. In particular, the near-horizon geometry of k fivebranes, which is obtained from (2.4) by omitting the constant term in the harmonic function H , (2.5), is known to be valid for all $k \geq 2$ [20-22]. A corollary of this is that our assertion that the brane configuration of figure 2 develops a localized tachyon for $\Delta x < \pi l$, with l given by (2.3), is exact as well. Indeed, regardless of the values of y_1 and y_2 in figure 2, the $D4$ and $\overline{D4}$ -branes always stretch all the way down the semi-infinite fivebrane throat. The linear dilaton description of this throat [20] leads to the mass formula (3.16) which is thus exact.

In the near-horizon, linear dilaton geometry, the phase structure of the full string theory must agree with our DBI analysis of the case $y < l$ in subsection 3.2.1. To recapitulate,

the system undergoes a second order phase transition at $\Delta x = \pi l$. In the broken phase the shape of the $D4$ -branes is a piece of the hairpin brane⁶ of [30,31], which exists only for $\Delta x < \pi l$. As Δx approaches πl from below, the bottom of the hairpin approaches the fivebranes and the solution smoothly connects to that of figure 2. The order parameter behaves qualitatively as in figure 9. The fact that the hairpin brane is an exact solution of the classical open string equations of motion implies that the above statements are valid for all $k \geq 2$.

Another part of our analysis that is valid for all k , including $k = 1$, involves the behavior of the solution of figure 6 for $y_i \gg l$ (in the full, asymptotically flat geometry (2.4)). In this regime the solution of figure 6 is located entirely in the large y region. Indeed, even for the largest separation Δx for which it exists, corresponding to $\theta = \theta_0$ (3.19), the minimal value of y along the $D4$ -brane, y_m (3.20), is in this case large. Therefore, the DBI approximation is valid not necessarily because k is large but because the D -brane sits in a region of small curvature at large y .

Thus, the fact that for large y_i the system undergoes a strongly first order phase transition at a value of Δx approximately given by (3.11), (3.23), is a reliable outcome of our analysis. As y_i decrease towards l the phase transition becomes less strongly first order. An interesting question is whether there is a critical value of y below which the transition becomes second order, as was found in our DBI analysis, or whether the transition remains first order for arbitrarily small y due to $1/k$ corrections, only becoming second order as $y \rightarrow 0$.

We believe that for small y the phase transition must be second order, as in the DBI analysis. Indeed, consider the brane configuration of figures 2, 6 for $y_1 = y_2 = y \ll l$. Since the configuration of figure 2 is locally stable only for $\Delta x \geq \pi l$, any first order transition would have to occur at a value of Δx larger than πl . This means that there must be a smooth solution of the sort depicted in figure 6 for Δx slightly larger than πl . At the same time, this solution should extend into the region in which the fivebrane geometry is well approximated by the linear dilaton one. Hence it has to look locally like the hairpin brane, which has by construction $\Delta x < \pi l$.

To summarize, it appears that the DBI analysis of this section captures the correct phase structure of the full classical string theory in our background, and describes correctly many quantitative features as well. Some parameters, such as the value of y at which the

⁶ Or, more precisely, of its $N = 2$ superconformal generalization discussed in [26,33,32].

phase transition goes from being first order to second order, can receive α' corrections. Others, such as the value of Δx at which the configuration of figure 2 ceases to exist, are given precisely by the DBI analysis. It is also important to remember that the discussion here is entirely classical. We will see below that quantum corrections give rise to qualitatively new features.

4. Gauge theory analysis at small Δx

In the previous section we studied the dynamics of the brane configuration of figure 2 in classical string theory. It is interesting to analyze the quantum (g_s) corrections to the resulting picture. For small Δx this can be done by using the low energy field theory on the branes, which is well understood. In this section we will review the dynamics of this field theory. In the next section we will suggest the generalization for larger Δx .

We start with the brane configuration of figure 5. For simplicity, we restrict the discussion to the case where the number of NS -branes is $k = 1$.⁷ The low energy dynamics of this brane configuration is described by an $N = 1$ supersymmetric gauge theory with gauge group

$$G_{\text{mag}} = U(N_2 - N_1) \times U(N_2) \equiv U(\tilde{N}_1) \times U(N_2) . \quad (4.1)$$

The gauge couplings of the two factors are given by

$$\tilde{\alpha}_1 = \frac{g_s l_s}{y_1} , \quad \tilde{\alpha}_2 = \frac{g_s l_s}{y_2 - y_1} . \quad (4.2)$$

In particular, in the regime described in the previous sections, small g_s and fixed y_i/l_s , the classical gauge theory is weakly coupled. By tuning y_1 and y_2 one can arrange for one of the gauge couplings to be much larger than the other, so that only one of the factors in the gauge group (4.1) is important.

In addition to the gauge multiplets, the gauge theory contains the following chiral superfields: an adjoint of $U(N_2)$, Φ_2 (which is proportional to M (2.13)), and bifundamentals q, \tilde{q} in the $(\tilde{N}_1, \overline{N}_2)$ and (\tilde{N}_1, N_2) , respectively. The superpotential is given by

$$W = h\Phi_2\tilde{q}q , \quad (4.3)$$

⁷ It is possible to generalize it to larger k by using the relevant gauge theory for that case [1]. This is necessary for making contact with the analysis of section 3, much of which assumes that $k > 1$.

where

$$h^2 = \tilde{\alpha}_2 . \quad (4.4)$$

The deformation of figure 5 that appears in figures 2, 3, corresponding to a relative displacement of the NS' -branes in the x direction, is described in the above gauge theory by an addition of a linear term to the superpotential (4.3). Following [10,13] we parametrize it as follows:

$$W = h\Phi_2\tilde{q}q - h\mu^2\text{Tr}\Phi_2 . \quad (4.5)$$

The mass parameter μ is given in terms of g_s, l_s and Δx by (see eq. (2.11) in [13])

$$\mu^2 = -\frac{\Delta x}{2\pi g_s l_s^3} . \quad (4.6)$$

The above gauge theory is valid at energy scales well below a scale E_c which can be taken to be the lowest of m_s and the Kaluza-Klein scales $1/y_i$.

Classically, the F-term of Φ_2 in (4.5) leads to supersymmetry breaking via a mechanism that generalizes the O’Raifeartaigh model. Some of the components of Φ_2 get a mass in the process; some others give rise to pseudo-moduli, which have a classically flat potential. The supersymmetry breaking ground state is described in terms of branes by the configuration of figure 3 [11-13]. The pseudo-moduli correspond to translational modes of the $D4$ -branes stretched between the NS' -branes.

Quantum mechanically, two things happen. The potential of the pseudo-moduli ceases to be flat near the origin, and supersymmetric vacua appear at finite Φ_2 . When the coupling $\tilde{\alpha}_2$ in (4.2) is small, the analysis of these effects is identical to that of [10]. In particular, the mass of the pseudo-moduli is of order⁸ $h^2|\mu|$. The gauging of $U(N_2)$ leads to corrections to that analysis, but these are small if the dynamically generated scale,

$$\Lambda_2 = E_c \exp \left[-\frac{8\pi^2(y_2 - y_1)}{(2N_2 - \tilde{N}_1)g_s l_s} \right] , \quad (4.7)$$

is much smaller than the mass $h^2|\mu|$. This can be achieved by increasing y_2 , thereby decreasing the gauge coupling $\tilde{\alpha}_2$ (4.2).

The supersymmetric vacua occur at

$$\langle h\Phi_2 \rangle \simeq \left(\mu^{2\tilde{N}_1} \Lambda_1^{N_1 - 2\tilde{N}_1} \right)^{\frac{1}{\tilde{N}_1}} . \quad (4.8)$$

⁸ Equations (4.2), (4.4) and (4.6) imply that this mass is proportional to $\sqrt{g_s} = g_{\text{open}}$. This is consistent with the fact that it comes from one loop open string effects (*i.e.* the annulus).

We are interested, following [10], in the case $N_2 > 3\tilde{N}_1$, where the $U(\tilde{N}_1)$ factor in (4.1) is not asymptotically free. It becomes strongly coupled at the scale

$$\Lambda_1 = E_c \exp \left[\frac{8\pi^2 y_1}{(N_2 - 3\tilde{N}_1) g_s l_s} \right]. \quad (4.9)$$

In the regime of interest for our analysis this scale is much higher than E_c , so the gauge theory description breaks down when it is still weakly coupled. In particular, for the analysis of [10] to be valid, one must have

$$\langle h\Phi_2 \rangle \ll E_c. \quad (4.10)$$

Plugging in the values of the different parameters one finds that (4.10) implies that the gauge theory analysis is only valid in the regime where Δx is smaller than $\exp(-C/g_s)$ for some positive constant C .

We see that the DBI regime of section 3 is well outside the regime of validity of the gauge theory. The relevant description in this regime is in terms of brane dynamics in string theory, which provides a different UV completion of the non-asymptotically free magnetic gauge theory (4.1) than that of [10]. There, the UV theory is the electric theory (2.8) described in section 2. Here, it is the open+closed string theory in the background of figure 5 (and its deformations). However, in the regime of validity of the magnetic gauge theory (4.10), the vacuum structure is insensitive to the UV completion and the above analysis is valid.

5. Quantum effects at large Δx

In the previous section we analyzed the low energy dynamics of the full quantum theory corresponding to the brane configuration of figure 3 using the gauge theory description, which is valid for small Δx (or small m (2.11)). In this section we will discuss quantum effects in the regime studied classically in section 3, where Δx is of order l_s or larger, and g_s is very small. As we will see, a full analysis of this problem requires more work, but we will suggest a picture that incorporates the results of sections 3, 4 and interpolates between them.

An important phenomenon that is absent classically but needs to be taken into account in the quantum analysis is bending of the $NS5$ -branes [34]. Consider, for example,

the NS'_1 -brane in figure 2. The $N_1 \overline{D4}$ -branes ending on it are seen in the fivebrane world-volume theory as charged particles in the two remaining dimensions along the fivebrane,

$$w = x^8 + ix^9 . \quad (5.1)$$

Classically, the NS'_1 -brane is located at a particular value of y , $y = y_1$. For finite g_s its location in y becomes a function of the distance from the fourbranes, $|w|$ [34]. Asymptotically, for large $|w|$, it behaves like

$$y \simeq N_1 g_s l_s \ln \frac{|w|}{l_s} . \quad (5.2)$$

There are also some other fields on the fivebrane that behave non-trivially due to the presence of the $D4$ -branes, but we will not discuss them in detail.

The bending (5.2) is in the y direction since this direction lies along the $D4$ -branes and transverse to the NS' -brane. Thus, it depends on the orientation of the $D4$ -branes (as well as on their number). This means that in going from the configuration of figure 2 to that of figure 3, which as we argued above is sometimes energetically favorable, the asymptotic shape of the NS' -branes at large $|w|$ changes by an infinite amount. At first sight this seems to suggest that such transitions are dynamically impossible, and one should take the shape of the fivebranes at infinity as given when studying these systems [13].

Our view is that processes in which the asymptotic bending of the fivebranes changes *are* dynamically allowed. Consider for example the case (analyzed classically in section 3) where the two NS' -branes are located at $y_1 = y_2 = y \gg l$, and the distance between them, Δx , is in the range $\sqrt{2}\pi l_s < \Delta x < \pi l$. In this case, we saw that the open string tachyon leads to a localized instability of the $D - \overline{D}$ system in the near-horizon region of the NS -branes. Indeed, while its mass squared in the flat space far from the fivebranes, (3.17), is positive, the near-horizon mass squared (3.16) is negative.

If the $D4$ -branes and antibranes were parallel and extended all the way to infinity in the y direction, the above localized tachyon would condense, and as a result the branes and antibranes would connect and move off to large y . In the system of figure 2, the initial stage of the process of tachyon condensation has to be the same, since the dynamics near the NS -branes has no way of knowing that at some large value of y the $D4$ -branes and antibranes are attached to other branes. Thus, one expects the tachyon localized near the NS -branes to start condensing, leading to a reconnection of the D -branes deep in the throat of the fivebranes. The part of the D -branes where they attach to the NS' -branes is initially not influenced by the reconnection.

At some point in the process of tachyon condensation, when the D-branes already have a shape similar to that of figure 6, this part of the D-branes is sufficiently deformed that the NS' -branes backreact. They develop a kink which interpolates between the behavior (5.2) and the one appropriate for the smooth connected solution of figure 6. This kink moves off to infinity such that at late times the full configuration looks like that of figure 6, with the bending appropriate for the D-brane shape. Of course, this process takes an infinite amount of time, but for an observer localized near the intersection this is irrelevant, since the kink leaves the vicinity of the intersection very rapidly.

Some comments about the preceding discussion are in order:

- (1) In section 3 we found that in some cases the instability of a brane configuration such as that of figure 2 is non-perturbative and requires tunneling through a barrier. The discussion above should apply to these as well. Consider for example the case where the NS' -branes are at a y slightly larger than l , and the distance between the $D4$ and $\overline{D4}$ -branes, Δx , is slightly above πl . We saw in section 3 that in this case the configuration of figure 2 is a local minimum of the classical energy and is separated by a small potential bump from the true minimum, which is the configuration of figure 6 (the energy landscape in this case is qualitatively depicted in figure 11). One can again choose the parameters such that the whole process of tunneling takes place in the near-horizon region, and only later is the information that it occurred communicated to the fivebranes. For these kinds of non-perturbative instabilities one expects a similar picture to the one described above.
- (2) Above we discussed cases in which the open string instability occurs deep inside the near-horizon region of the fivebranes and the backreaction of the NS' -branes is a late time effect. We expect the basic picture to hold in general. The open string instability is always localized near the intersection of the various branes. Its resolution is the leading dynamical effect, and once it occurs the bulk of the fivebranes reacts to the new structure at the intersection in the way described above.
- (3) The preceding discussion is very reminiscent of what happens in the process of localized closed string tachyon condensation on non-compact orbifolds (see *e.g.* [35,36]). Just like here the brane configuration can be characterized by a particular shape of the $NS5$ -branes at infinity, there the geometry is a cone of some particular opening angle infinitely far from the tip. The analogs of open string instabilities in that case are tachyons localized at the tip (which come from twisted sectors of the orbifold CFT).

The asymptotic boundary conditions at infinity can change under condensation of these tachyons, just like the asymptotic shape of the fivebranes in our examples.

In the remainder of this section we will use the results of sections 3, 4 to propose a possible form for the phase diagram of the model corresponding to the brane configurations of figures 2 – 6. Our basic picture is summarized in figure 14 where we incorporate the distinction between the cases⁹ $y > l$ and $y < l$ found in section 3.

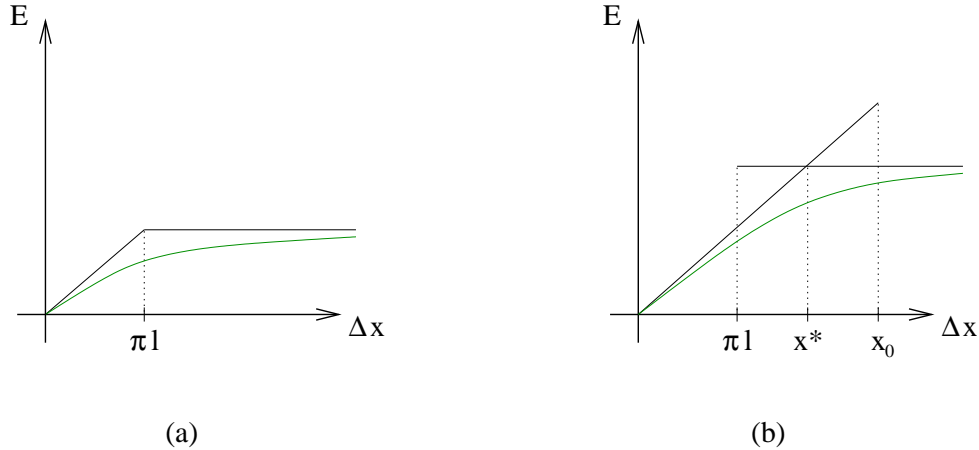


Fig. 14: The phase diagram of the intersecting brane model of figures 2 – 6 for $y < l$ (a), and $y > l$ (b). In figure 14b we use the notation $x^* \equiv \Delta x(\theta^*)$, $x_0 \equiv \Delta x(\theta_0)$.

The horizontal black lines in figures 14a,b correspond to the brane configuration of figure 2. A result from section 3 which is incorporated in the figure is that this configuration is a local minimum of the effective action only for $\Delta x > \pi l$. The diagonal black lines in figures 14a,b correspond to the configuration of figure 6. For $\Delta x < \pi l$ this configuration is the only minimum of the effective action. For $\Delta x > \pi l$ the situation is different for $y < l$ and $y > l$. In the former case this solution ceases to exist in this regime. Thus, the transition at $\Delta x = \pi l$ is second order, as explained in section 3 (see figure 9) and is indicated in figure 14a. For $y > l$ this solution remains a local minimum of the effective action in a finite range of $\Delta x > \pi l$, as indicated in figure 14b. The transition at $\Delta x = x^*$ is first order (see figure 13).

Both the horizontal and the diagonal black lines in figure 14, which were found in the classical analysis of section 3, describe non-supersymmetric brane configurations, so supersymmetry is broken in this system, at least classically. An important question is

⁹ As mentioned in subsection 3.4, it is possible that in the full open string theory, beyond the DBI approximation, the critical value of y is shifted from l by $1/k$ corrections.

whether this is the case in the quantum theory as well. The gauge theory analysis of section 4 suggests that the answer is no. This analysis is valid in a small region near the origin in figure 14, and it suggests that in that region there exists a lower energy supersymmetric configuration, which we denote in figure 14 by the curved magenta line. That line was shown above to exist only in a small vicinity of the origin, but it is natural to expect that it extends to all values of Δx . It approaches one of the non-supersymmetric configurations corresponding to the straight black lines in the two extreme regions $\Delta x \rightarrow 0, \infty$.

As $\Delta x \rightarrow 0$ this can be understood from the gauge theory analysis of [10] and section 4. In this region the mass parameter m (2.11) is very small and the supersymmetric ground state becomes almost indistinguishable from the meta-stable non-supersymmetric one. The latter is described in terms of branes by the configuration of figures 3, 6 [11-15].

As $\Delta x \rightarrow \infty$, figure 14 suggests that the supersymmetric ground state approaches the brane configuration of figure 2 where the separation between the $D4$ and $\overline{D4}$ -branes goes to infinity. This is physically reasonable – while the configuration of figure 2 is not supersymmetric, in the limit $\Delta x \rightarrow \infty$ it approaches one in which the dynamics of the $D4$ -branes is decoupled from that of the $\overline{D4}$ -branes. The low energy theory for large Δx is essentially the same for the non-supersymmetric brane configuration of figure 2, and the supersymmetric one of figure 4a. Both reduce to $N = 1$ SYM with gauge group $U(N_1) \times U(N_2)$ and no light matter.

We stress again that we have not proven that the supersymmetric ground state described by the curved magenta line in figure 14 exists beyond the regime of small Δx where one can establish its existence using gauge theory. It is not surprising that this is a subtle problem. Indeed, translating the gauge theory analysis to string theory language, the supersymmetric ground state should be highly quantum – its existence should be due to non-perturbative effects in g_s . Classically, such a vacuum does not exist. Furthermore, in order to get to it in the field space of the brane theory, one has to turn on fields that are non-geometric in the configurations of figures 2, 3, etc. Nevertheless, we expect that it should be possible to find this ground state directly in string theory. The two main reasons for our belief in this are the following:

- (1) The existence of a supersymmetric ground state at small Δx follows from the field theory analysis and it would be surprising if it ceased to exist at a finite value of Δx .
- (2) The work on brane constructions in the late 1990's reviewed in [1] seems to suggest that the low energy behavior behaves smoothly as one takes NS' -branes past NS -branes in configurations such as that of figure 4. This is supposed to be the reflection

of Seiberg duality in string theory [23]. Since in the electric brane configuration of figure 4 a supersymmetric ground state exists, one would expect the same to be true in the magnetic one of figures 2, 3.

A related point is that the phase structure we found is very similar to what is expected in gauge theory [10], despite the fact that in our regime of parameter space the gauge theory analysis is not valid. In particular, in [10] it was pointed out that as one increases the mass m (2.11), the meta-stable state becomes less and less long-lived, and eventually it disappears for sufficiently large m . Establishing this in gauge theory is not easy since it involves understanding the theory in a regime where there is no weakly coupled description.

In our analysis we found precisely the same behavior in the DBI approximation (which, as mentioned above, is valid in a different regime in the parameter space of brane configurations). Indeed, in figure 14 the meta-stable state, which is described by the diagonal black line in figures 14a,b, ceases to exist above a certain critical value. Moreover, the state it decays to has the same qualitative features as the one in [10]. Unlike the gauge theory regime, here one can analyze the system all the way to the point where the meta-stable state ceases to exist and beyond. This is a common situation in string theory: in one regime understanding the dynamics involves solving a non-trivial quantum field theory problem while in another one can analyze similar physics using classical string theory.

6. Discussion

In this paper we studied the phase structure of the brane system of figures 2, 3 as a function of the parameters defining the brane configuration. Most of our analysis was in the context of classical string theory in the regime where all distances in figures 2, 3 are kept finite in the limit $g_s \rightarrow 0$. We found that the system exhibits first and second order phase transitions in different regions of its parameter space.

We also discussed a different region in parameter space, which can be studied using an effective low energy gauge theory. In that region, we saw (following [10]) that quantum effects lead to additional vacua that preserve supersymmetry. The classical vacua become unstable, but are parametrically long-lived in the limit $g_s \rightarrow 0$.

Much of the physics of the brane configuration we analyzed remains to be understood. For example, it would be interesting to analyze the spectrum of excitations of the configuration of figure 6. Classically, this configuration is the ground state of the system for sufficiently small Δx , and in some cases (for $y > l$) is locally stable for a range of larger

values of Δx as well. Its low lying excitations can be analyzed by expanding the DBI action about the solution (3.2), as is familiar from studies of the Sakai-Sugimoto model [16] and other systems.

Perhaps the most interesting open problem is to understand whether the phase diagram of figure 14 is correct, and the supersymmetric ground states that exist in gauge theory persist for large Δx , where the gauge theory analysis is invalid. In gauge theory, the existence of these supersymmetric ground states is due to non-perturbative effects. If the same is true in the stringy (large Δx) regime, it is important to identify the relevant quantum effects and provide a good description of the supersymmetric vacua.

There are many natural generalizations of the brane configurations studied here. For example, replacing the NS'_2 -brane by N_2 $D6$ -branes stretched in (0123789) leads to the brane configuration corresponding to the magnetic dual of supersymmetric QCD with gauge group $U(N_1)$ and N_2 chiral superfields in the fundamental representation [23]. The separation of the NS'_1 -brane and $D6$ -branes in the x direction, that in gauge theory leads to meta-stable non-supersymmetric vacua [10], was discussed using branes in [11-15].

Our DBI analysis is applicable to this case as well since it does not depend on what the $D4$ -branes are ending on. In fact, this case is in some ways better behaved since the quantum brane bending effects (5.2) are smaller. In particular, the bending of the $D6$ -branes due to the $D4$ -branes ending on them goes to zero asymptotically. The classical string theory analysis of section 3 leads in this case to a picture very reminiscent of that of [10]. The phase diagram is again expected to be given by figure 14. The origin of the supersymmetric ground state is again not obvious, and it would be interesting to understand it better.

One can also consider the system in which the NS'_1 -brane is replaced by $D6$ -branes as well. The DBI analysis is still the same, but in this case there is no reason to expect non-trivial quantum dynamics to restore supersymmetry. Indeed, the low energy theory on the $D4$ -branes is in this case weakly coupled, and there are no large bending effects of the sort (5.2), since there are no longer any NS' -branes.¹⁰

Many other generalizations are suggested by the work on supersymmetric brane constructions reviewed in [1]. For example, the original work of [37] involved $D3$ -branes (rather than $D4$ -branes) suspended between $NS5$ -branes, and led to new insights into

¹⁰ The NS -branes play a very different role in our construction. For example, for $N_1 = N_2$ the total charge on them is zero, so asymptotically, for large (x^4, x^5) , they retain their classical shape.

2 + 1 dimensional gauge dynamics. It is natural to consider similar generalization in non-supersymmetric setups such as those studied in this paper.

As mentioned in the introduction, a class of related constructions involves branes and antibranes wrapping different cycles of non-compact CY manifolds. An example analyzed in [5,6] is the surface

$$y^2 = W'(x)^2 + uv , \tag{6.1}$$

with

$$W'(x) = (x - a_1)(x - a_2) . \tag{6.2}$$

This non-compact manifold can be thought of as two adjacent conifold singularities located at $x = a_1, a_2$. One can resolve each conifold by blowing up certain two-spheres in the geometry, and wrap $D5$ and $\overline{D5}$ -branes (which are also stretched in the usual Minkowski spacetime $\mathbb{R}^{3,1}$), respectively, around them.

The non-compact CY (6.1), (6.2) is related by T-duality [7-9] to a background which contains an $NS5$ -brane wrapped around the surface

$$y^2 = W'(x)^2 . \tag{6.3}$$

This is actually two fivebranes wrapped around the surfaces $y = \pm W'(x)$ in the \mathbb{C}^2 labeled by the complex coordinates (x, y) . The ten dimensional target space of type II string theory contains this \mathbb{C}^2 , the physical Minkowski spacetime, $\mathbb{R}^{3,1}$, and two additional dimensions, in which the two fivebranes can be separated. The $D5$ -branes and antibranes of [5,6] correspond in this description to $D4$ -branes and antibranes that are stretched between the two $NS5$ -branes, the $D4$ -branes at $x = a_1$ and the $\overline{D4}$ -branes at $x = a_2$.

From the perspective of our discussion, this system is simpler to understand than the one of figure 2. The branes and antibranes are locally stable, as in our case, but they can still annihilate by first increasing their energy. For example, if the number of $D4$ and $\overline{D4}$ -branes are equal, their ends on one of the $NS5$ -branes can approach each other and reconnect, such that the D -branes turn into a single stack both of whose ends lie on the other fivebrane. They can then shrink to zero size and disappear.

Thus, some of the non-trivial aspects of the analysis above are absent in this case. The classical ground state of the model is the supersymmetric state with no D -branes, as opposed to our case where it was one of the non-supersymmetric configurations of figures 2 or 6, depending on the parameters. The semiclassical phase diagram is simpler, and in particular the phase transitions we found are absent. Nevertheless, one can hope that

some of the techniques that were used to study that system can shed additional light on the one considered here and generalizations thereof.

Acknowledgements: We thank A. Parnachev for discussions. This work is supported in part by the BSF – American-Israel Bi-National Science Foundation. The work of AG is supported in part by the center of excellence supported by the Israel Science Foundation (grant No. 1468/06), EU grant MRTN-CT-2004-512194, the DIP grant H.52, and the Einstein Center at the Hebrew University. The work of DK is supported in part by DOE grant DE-FG02-90ER40560 and the National Science Foundation under Grant 0529954. AG thanks the EFI at the University of Chicago for hospitality. DK thanks the Weizmann Institute and Hebrew University.

References

- [1] A. Giveon and D. Kutasov, “Brane dynamics and gauge theory,” *Rev. Mod. Phys.* **71**, 983 (1999) [arXiv:hep-th/9802067].
- [2] O. Aharony, S. S. Gubser, J. M. Maldacena, H. Ooguri and Y. Oz, “Large N field theories, string theory and gravity,” *Phys. Rept.* **323**, 183 (2000) [arXiv:hep-th/9905111].
- [3] H. Ooguri and Y. Ookouchi, “Landscape of supersymmetry breaking vacua in geometrically realized gauge theories,” *Nucl. Phys. B* **755**, 239 (2006) [arXiv:hep-th/0606061].
- [4] R. Argurio, M. Bertolini, S. Franco and S. Kachru, “Gauge / gravity duality and meta-stable dynamical supersymmetry breaking,” arXiv:hep-th/0610212.
- [5] M. Aganagic, C. Beem, J. Seo and C. Vafa, “Geometrically induced metastability and holography,” arXiv:hep-th/0610249.
- [6] J. J. Heckman, J. Seo and C. Vafa, “Phase Structure of a Brane/Anti-Brane System at Large N,” arXiv:hep-th/0702077.
- [7] H. Ooguri and C. Vafa, “Two-Dimensional Black Hole and Singularities of CY Manifolds,” *Nucl. Phys. B* **463**, 55 (1996) [arXiv:hep-th/9511164].
- [8] D. Kutasov, “Orbifolds and Solitons,” *Phys. Lett. B* **383**, 48 (1996) [arXiv:hep-th/9512145].
- [9] A. Giveon, D. Kutasov and O. Pelc, “Holography for non-critical superstrings,” *JHEP* **9910**, 035 (1999) [arXiv:hep-th/9907178].
- [10] K. Intriligator, N. Seiberg and D. Shih, “Dynamical SUSY breaking in meta-stable vacua,” *JHEP* **0604**, 021 (2006) [arXiv:hep-th/0602239].
- [11] H. Ooguri and Y. Ookouchi, “Meta-stable supersymmetry breaking vacua on intersecting branes,” *Phys. Lett. B* **641**, 323 (2006) [arXiv:hep-th/0607183].
- [12] S. Franco, I. Garcia-Etxebarria and A. M. Uranga, “Non-supersymmetric meta-stable vacua from brane configurations,” arXiv:hep-th/0607218.
- [13] I. Bena, E. Gorbatov, S. Hellerman, N. Seiberg and D. Shih, “A note on (meta)stable brane configurations in MQCD,” *JHEP* **0611**, 088 (2006) [arXiv:hep-th/0608157].
- [14] C. Ahn, “Brane configurations for nonsupersymmetric meta-stable vacua in SQCD with adjoint matter,” arXiv:hep-th/0608160.
- [15] R. Tatar and B. Wetenhall, “Metastable vacua, geometrical engineering and MQCD transitions,” arXiv:hep-th/0611303.
- [16] T. Sakai and S. Sugimoto, “Low energy hadron physics in holographic QCD,” *Prog. Theor. Phys.* **113**, 843 (2005) [arXiv:hep-th/0412141].
- [17] E. Antonyan, J. A. Harvey, S. Jensen and D. Kutasov, “NJL and QCD from string theory,” arXiv:hep-th/0604017.
- [18] E. Antonyan, J. A. Harvey and D. Kutasov, “The Gross-Neveu model from string theory,” arXiv:hep-th/0608149.

- [19] E. Antonyan, J. A. Harvey and D. Kutasov, “Chiral symmetry breaking from intersecting D-branes,” arXiv:hep-th/0608177.
- [20] C. G. Callan, J. A. Harvey and A. Strominger, “Supersymmetric string solitons,” arXiv:hep-th/9112030.
- [21] O. Aharony, M. Berkooz, D. Kutasov and N. Seiberg, “Linear dilatons, NS5-branes and holography,” JHEP **9810**, 004 (1998) [arXiv:hep-th/9808149].
- [22] O. Aharony, A. Giveon and D. Kutasov, “LSZ in LST,” Nucl. Phys. B **691**, 3 (2004) [arXiv:hep-th/0404016].
- [23] S. Elitzur, A. Giveon and D. Kutasov, “Branes and $N = 1$ duality in string theory,” Phys. Lett. B **400**, 269 (1997) [arXiv:hep-th/9702014].
- [24] S. Elitzur, A. Giveon, D. Kutasov, E. Rabinovici and A. Schwimmer, “Brane dynamics and $N = 1$ supersymmetric gauge theory,” Nucl. Phys. B **505**, 202 (1997) [arXiv:hep-th/9704104].
- [25] N. Seiberg, “Electric - magnetic duality in supersymmetric nonAbelian gauge theories,” Nucl. Phys. B **435**, 129 (1995) [arXiv:hep-th/9411149].
- [26] D. Kutasov, “D-brane dynamics near NS5-branes,” arXiv:hep-th/0405058.
- [27] N. Itzhaki, D. Kutasov and N. Seiberg, “Non-supersymmetric deformations of non-critical superstrings,” JHEP **0512**, 035 (2005) [arXiv:hep-th/0510087].
- [28] D. Kutasov, “A geometric interpretation of the open string tachyon,” arXiv:hep-th/0408073.
- [29] A. Giveon and D. Kutasov, “Fundamental strings and black holes,” arXiv:hep-th/0611062.
- [30] S. L. Lukyanov, E. S. Vitchev and A. B. Zamolodchikov, “Integrable model of boundary interaction: The paperclip,” Nucl. Phys. B **683**, 423 (2004) [arXiv:hep-th/0312168].
- [31] S. L. Lukyanov and A. B. Zamolodchikov, “Dual form of the paperclip model,” Nucl. Phys. B **744**, 295 (2006) [arXiv:hep-th/0510145].
- [32] D. Kutasov, “Accelerating branes and the string / black hole transition,” arXiv:hep-th/0509170.
- [33] Y. Nakayama, Y. Sugawara and H. Takayanagi, “Boundary states for the rolling D-branes in NS5 background,” JHEP **0407**, 020 (2004) [arXiv:hep-th/0406173].
- [34] E. Witten, “Solutions of four-dimensional field theories via M-theory,” Nucl. Phys. B **500**, 3 (1997) [arXiv:hep-th/9703166].
- [35] A. Adams, J. Polchinski and E. Silverstein, “Don’t panic! Closed string tachyons in ALE space-times,” JHEP **0110**, 029 (2001) [arXiv:hep-th/0108075].
- [36] J. A. Harvey, D. Kutasov, E. J. Martinec and G. W. Moore, “Localized tachyons and RG flows,” arXiv:hep-th/0111154.
- [37] A. Hanany and E. Witten, “Type IIB superstrings, BPS monopoles, and three-dimensional gauge dynamics,” Nucl. Phys. B **492**, 152 (1997) [arXiv:hep-th/9611230].